Observation of modulational instability in discrete media with self-defocusing nonlinearity

Milutin Stepić, Christian Wirth, Christian E. Rüter, and Detlef Kip

Institute of Physics and Physical Technology, Clausthal University of Technology,
D-38678 Clausthal-Zellerfeld, Germany

We report what we believe is the first observation of modulation instability in the anomalous-diffraction regions of a photonic lattice. The experiments were carried out in a 1D waveguide array fabricated in a lithium niobate crystal displaying the photovoltaic self-defocusing nonlinearity, and our results are confirmed numerically by simulating the nonlinear beam propagation. © 2006 Optical Society of America
    OCIS codes: 190.0190, 190.3100, 190.5330.

Modulational instability (MI) is a nonlinear wave phenomenon that manifests itself as the breakup of an extended state of a system into a train of highly localized states. In homogeneous nonlinear media, the extended state is a plane wave, which, under the action of a self-focusing nonlinearity, breaks up spontaneously into multiple filaments. In periodic systems, the extended states are Floquet–Bloch (FB) modes, which can also undergo MI: FB modes exhibiting normal diffraction experience MI in the presence of self-focusing, whereas FB modes displaying anomalous diffraction break up under self-defocusing. Very often, the breakup process ends up in a train of equally spaced solitons, with the spacing being inversely proportional to the spatial frequency of the highest nonlinear gain. As such, the MI process is intimately related to the formation of solitons.[1] MI is considered a universal phenomenon that appears in many branches of nonlinear science. For example, MI has been investigated in neutrino–antineutrino interactions,[2] pulsar plasma,[3] atomic vapors,[4] laser–plasma interaction,[5] easy-axis antiferromagnetic chains,[6] and Bose–Einstein condensates.[7,8] In the optics case, MI has been observed in fibers,[9] liquid crystals,[10] nonlinear cavities,[11] photorefractive crystals,[12–14] quadratic media,[15] and by using spatially incoherent light beams.[16,17] The existence of discrete MI has been suggested in Ref. 18.

In this Letter we explore MI in a periodic nonlinear optical lattice.[18–24] Periodic structures such as waveguide arrays and photonic crystal fibers can now be rather easily fabricated, enabling the investigation of various associated linear and nonlinear effects such as FB oscillations,[25] discrete diffraction,[26] and lattice or gap solitons.[27] The linear modes in such periodic lattices are extended FB modes, with a transmission spectrum consisting of allowed bands separated by forbidden gaps. In the nonlinear case, the modes experience instabilities and break up into spatially modulated patterns of high regularity.

MI may be regarded as the first step toward energy localization in 1D lattices with self-focusing Kerr nonlinearity.[18,22] The first experimental observation of discrete MI in AlGaAs arrays that exhibit cubic nonlinearity was reported during 2004.[19] On the other hand, again in the Kerr case, working at the edge of the first Brillouin zone, Kivshar proposed that plane-wave solutions of staggered form (adjacent elements of the array are out of phase) can also experience MI, provided that the array exhibits a self-defocusing nonlinearity.[23] Here we confirm experimentally the theoretical prediction of the existence of MI in the first band of a 1D periodic system with defocusing saturable nonlinearity that has been reported recently.[24] In general, saturation has a stabilizing role: it increases the threshold for the onset of MI and decreases the MI gain.

Permanent 1D waveguide arrays are fabricated using x-cut lithium niobate wafers of congruently melting composition. A typical sample size is 1 mm $\times$ 17 mm $\times$ 7.8 mm along the crystallographic x, y, and z axes, respectively.[28] The ferroelectric c axis coincides with the z axis, while the channels are directed along the y axis. Waveguides with a width of 4 μm that are separated by 3.6 μm (lattice period Λ = 7.6 μm) are fabricated by Ti indiffusion in a sample that is additionally surface doped by diffusion of Fe to enhance the photorefractive effect. The resulting nonlinearity is of a saturable type, which results from both the relatively high dark conductivity of the sample ($\sigma_d \approx 10^{-13}$ VA^{-1} m^{-1}) and the limited number of electron traps. Each separate channel forms a single-mode waveguide for TE polarized light. The resulting refractive index profile of our sample at an effective depth (measured from the surface), where the mode intensity has its maximum, is given by $n(z) = n_e + \Delta n(z) = 2.2420 + 0.0063 \cos^2(\pi z/\Lambda)$. The calculated bandgap diagram of the waveguide array in which the propagation constant $\beta' = \beta - 2\pi n_e/\Lambda$ is related to the transverse Bloch wavenumber k_z is presented in Fig. 1. Regions of anomalous diffraction in the first band are hatched and marked with arrows. In these regions discrete MI may occur as a result of the interplay between self-defocusing nonlinearity and anomalous diffraction. Note that at the edges of the first Brillouin zone in the second band the diffraction is normal, disabling the occurrence of this instability.

We excited FB modes in the array by use of the prism coupling method shown in Fig. 2, with green light ($\lambda = 514.5$ nm). Here the propagation constant β of a FB mode may be chosen by variation of coupling
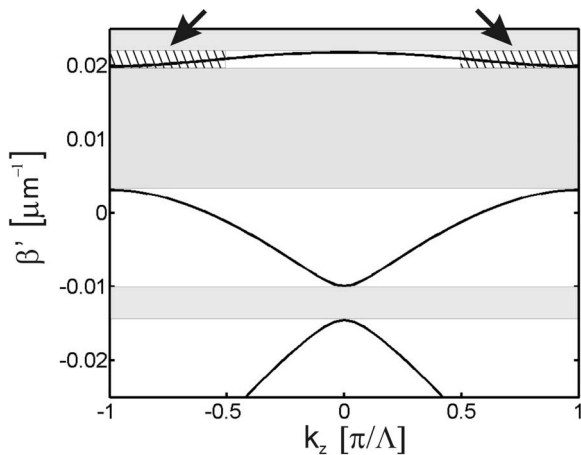
Fig. 1. Dispersion relation of our 1D waveguide array. The shaded regions are gaps in which light cannot propagate. The arrows point to the regions of anomalous diffraction within the first band. The value $\beta' = 0$ is given relative to the propagation constant of a substrate mode.
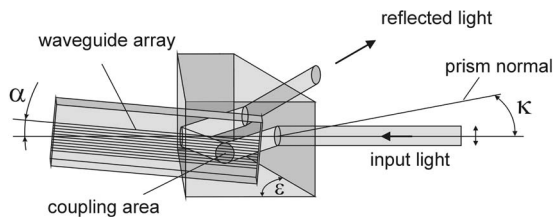
Fig. 2. Geometry of the prism coupler setup used to excite certain FB modes of the 1D waveguide array.

angle κ, while transverse wave vector k_z can be determined by an angle α between the directions of input light and waveguide array [$\alpha = \arcsin(|k_z|\lambda/2\pi n_{\text{eff}})$].[29] The general advantage of this method is a well-defined excitation of desired modes of the array. Also, it represents an easy tool to analyze the excited FB mode spectra, which may result from a nonlinear interaction inside the sample, by using a similar prism for outcoupling of the light. Here we use only one rutile prism with internal angle ϵ for excitation of FB modes while the intensity patterns on the end facet of the sample are monitored by a CCD camera.

Experimentally we excited all 250 channels of our sample (power per channel, 0.5 μW). In Fig. 3 data collected by the CCD camera that images the rear facet of the array after 15 mm of propagation are given. We monitored the temporal evolution of light intensity in the selected part of the array for the first and second bands, respectively, where we take advantage of the fact that the photovoltaic nonlinearity grows until saturation as a function of time. As expected from theory, we did not observe MI at the base of the Brillouin zone in the first band where all channels are excited in phase. Then the phase difference between adjacent elements of the array was adjusted to be approximately π by fixing the angle α to $\alpha = 0.9°$. The respective pictures for times $t = 0$ monitor the linear case where no nonlinearity has built up yet (the intensity modulations still observable for $t = 0$ are weak and result from varying coupling efficiency

of the prism coupler and small sample defects). In the first band one may notice focusing of light and formation of localized staggered solitonlike structures that comprise approximately four channels, with a buildup time of typically 2–5 min. For longer illumination times finer intensity structures appear, probably as an outcome of nonlinear coupling to higher FB modes and interference effects. Furthermore, an increase of the spatial frequency of the soliton trains with increasing input power is observed. On the other hand, in the second band there is no observable change in the light intensity distribution, however, nonlinear coupling to higher modes is observed as well. Please note that for the second band intensity maxima are laterally shifted, as now the light is guided between the waveguide channels. This is shown in Fig. 3, where results for the first 20 min of illumination are given, thus confirming the theoretical prediction of absent MI in the second band at the edge of the Brillouin zone.

To check these results we performed numerical simulations using a nonlinear beam propagation method (BPM). For this we used the parameters of our waveguide array and a saturable defocusing nonlinearity of the form $\Delta n = \Delta n_{\text{nl}} I/(I + I_d)$ with $\Delta n_{\text{nl}} = -0.000\,55$ and $r = I/I_d = 3$, where I_d is the dark irradiance and I is the light intensity. The parameters for the nonlinearity used here are typical for our LiNbO$_3$:Ti:Fe sample.[30] Figure 4 shows typical numerical results in which a pure nonlinear FB mode of the first band at the edge of the Brillouin zone is excited, together with some random noise. Here one may recognize a gradual disintegration of the excited mode and the formation of narrow localized states resembling trains of discrete solitons with a spatial frequency of approximately $\Omega = 0.125$ μm^{-1}, in good agreement with the experimental result. Here the width of a single maximum in the MI pattern coincides fairly well with the typical width of a single (staggered) soliton in a similar sample used in Ref. 28. On the other hand, if we launch the corresponding FB modes at the band edge of the second band, this mode propagates stably and MI is absent. For different nonlinearities Δn_{nl} and intensity ratios r, small variations in the observed spatial frequency are obtained for the first band as shown in Fig. 5, and a complete suppression of MI for very large values of r is also obtained.
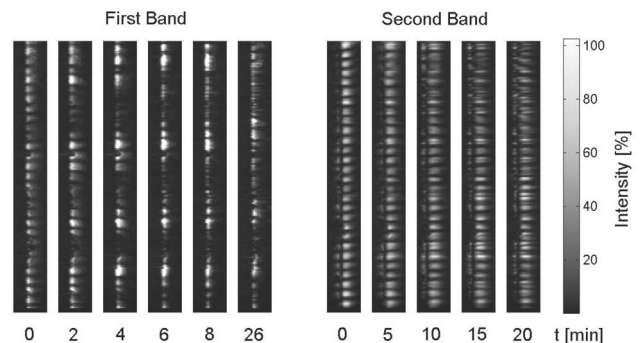
Fig. 3. Light intensity distribution I at the rear facet of the array within the first and second bands as a function of illumination time t.
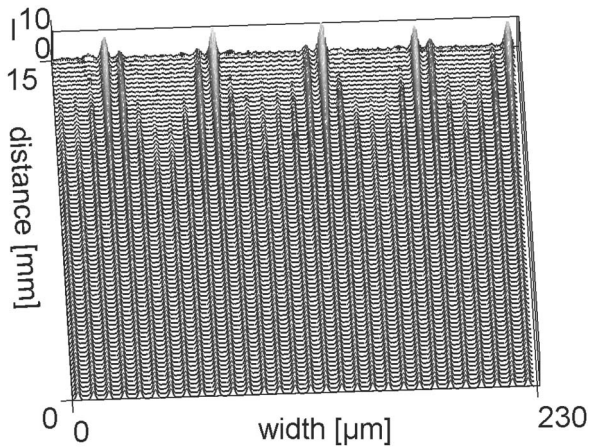
Fig. 4.   BPM simulation of MI in the first band of a nonlinear waveguide array with nonlinearity $\Delta n = \Delta n_{nl} I/(I+I_d)$ ($\Delta n_0 = -0.000\,55, I/I_d = 3$).
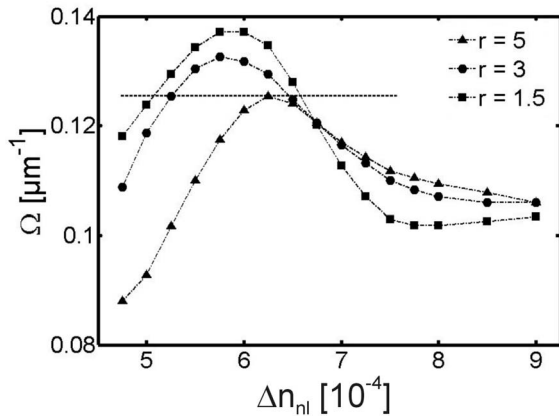
Fig. 5.   Spatial frequency Ω of MI in the first band obtained with BPM as a function of nonlinearity Δn_{nl} and for different intensity ratios r. The dotted horizontal line is the experimentally observed frequency in Fig. 4.

In conclusion, discrete MI of a staggered plane-wave solution within the first two bands of a permanent 1D waveguide array with self-defocusing nonlinearity is investigated both experimentally and numerically. In the first band, strong localization of intensity can be regarded as proof for the occurrence of MI at the edges of the first Brillouin zone, i.e., in the regime of anomalous diffraction. Finally, it is demonstrated that under the same nonlinear conditions MI does not develop in the second band where dispersion is normal.

References

1. G. I. Stegeman and M. Segev, Science **280**, 889 (1998).
2. M. Marklund, P. K. Shukla, G. Betschart, L. Stenflo, D. Anderson, and M. Lisak, J. Exp. Theor. Phys. **99**, 9 (2004).
3. G. Z. Machabeli, Q. Luo, S. V. Vladimirov, and D. B. Melrose, Phys. Rev. E **65**, 036408 (2002).
4. P. Gauthier, O. Gobert, M. Comte, D. L'Hermite, J. de Lamare, and D. Benisti, Phys. Rev. A **65**, 033804 (2002).
5. M. L. Begue, A. Ghizzo, P. Bertrand, E. Sonnendrucker, and O. Couland, J. Plasma Phys. **62**, 367 (1999).
6. R. Lai and A. J. Sievers, Phys. Rev. B **57**, 3433 (1998).
7. L. D. Carr and J. Brand, Phys. Rev. Lett. **92**, 040401 (2004).
8. K. E. Strecker, G. B. Partridge, A. G. Truscott, and R. G. Hulet, Nature **417**, 150 (2002).
9. A. Hasegawa, Opt. Lett. **9**, 288 (1984).
10. M. Peccianti, C. Conti, G. Assanto, A. DeLuca, and C. Umeton, Nature **432**, 733 (2004).
11. D. Gomila, R. Zambrini, and G.-L. Oppo, Phys. Rev. Lett. **92**, 253904 (2004).
12. M. D. Iturbe-Castillo, M. Torres-Cisneros, J. J. Sánchez-Mondragón, S. Chávez-Cerda, S. I. Stepanov, V. A. Vysloukh, and G. E. Torres-Cisneros, Opt. Lett. **20**, 1853 (1995).
13. M. I. Carvalho, S. R. Singh, and D. N. Christodoulides, Opt. Commun. **126**, 167 (1996).
14. A. V. Mamaev, M. Saffman, and A. A. Zozulya, Europhys. Lett. **35**, 25 (1996).
15. H. Fang, R. Malendevich, R. Schiek, and G. I. Stegeman, Opt. Lett. **25**, 1786 (2000).
16. M. Soljačić, M. Segev, T. Coskun, D. N. Christodoulides, and A. Vishwanath, Phys. Rev. Lett. **84**, 467 (2000).
17. D. Kip, M. Soljačić, M. Segev, E. Eugenieva, and D. N. Christodoulides, Science **290**, 495 (2000).
18. D. N. Christodoulides and R. I. Joseph, Opt. Lett. **13**, 794 (1988).
19. J. Meier, G. I. Stegeman, D. N. Christodoulides, Y. Silberberg, R. Morandotti, H. Yang, G. Salamo, M. Sorel, and J. S. Aitchinson, Phys. Rev. Lett. **92**, 163902 (2004).
20. Yu. S. Kivshar and M. Peyrard, Phys. Rev. A **46**, 3198 (1992).
21. H. G. Winful, R. Zamir, and S. Feldman, Appl. Phys. Lett. **58**, 1001 (1991).
22. I. Daumont, T. Dauxois, and M. Peyrard, Nonlinearity **10**, 617 (1997).
23. Yu. S. Kivshar, Opt. Lett. **18**, 1147 (1993).
24. A. Maluckov, M. Stepić, D. Kip, and Lj. Hadžievski, Eur. Phys. J. B **45**, 539 (2005).
25. T. Pertsch, P. Dannberg, W. Elflein, A. Brauer, and F. Lederer, Phys. Rev. Lett. **83**, 4752 (1999).
26. R. Morandotti, H. S. Eisenberg, Y. Silberberg, M. Sorel, and J. S. Aitchinson, Phys. Rev. Lett. **86**, 3296 (2001).
27. J. W. Fleischer, G. Bartal, O. Cohen, T. Schwartz, O. Manela, B. Freedman, M. Segev, H. Buljan, and N. K. Efremidis, Opt. Express **13**, 1780 (2005).
28. F. Chen, M. Stepić, C. E. Rüter, D. Runde, D. Kip, V. Shandarov, O. Manela, and M. Segev, Opt. Express **13**, 4314 (2005).
29. R. Zengerle, J. Mod. Opt. **34**, 1589 (1987).
30. J. Hukriede, D. Kip, and E. Krätzig, Appl. Phys. B **66**, 333 (1998).